Fast one-dimensional photonic crystal modulators for the terahertz range

L. Fekete,[1] F. Kadlec,[1] H. Němec[2] and P. Kužel[1]*

[1]*Institute of Physics, Academy of Sciences of the Czech Republic, Na Slovance 2, 182 21 Prague 8, Czech Republic*
[2]*Chemical Center, Lund University, Getingevägen 60, 222 41 Lund, Sweden*
kuzelp@fzu.cz

Abstract: Optically controlled one-dimensional photonic crystal structures for the THz range are studied both theoretically and experimentally. A GaAs:Cr layer constitutes a defect in the photonic crystals studied; its photoexcitation by 800 nm optical femtosecond pulses leads to the modulation of the THz beam. Since the THz field can be localized in the photoexcited layer of the photonic crystal, the interaction between photocarriers and THz light is strengthened and yields an appreciable modulation of the THz output beam even for low optical pump fluences. Optimum resonant structures are found, constructed and experimentally studied. The dynamical response of these elements is shown to be controlled by the lifetime of THz photons in the resonator and by the free carrier lifetime. The time response of the structures studied is shorter than 330 ps.

OCIS codes: (160.5140) Photoconductive materials; (300.6270) Spectroscopy, far infrared; (300.6530) Spectroscopy, ultrafast; (230.1150) All-optical devices; (230.4110) Modulators

References and links

1. B. Ferguson and X.-C. Zhang, "Materials for terahertz science and technology," Nature materials **1**, 26 (2002).
2. M. Koch, "Terahertz Technology: A Land to Be Discovered," Opt. Photon. News **18 (3)**, 20 (2007).
3. A. Hirata, T. Kosugi, H. Takahashi, R. Yamaguchi, F. Nakajima, T. Furuta and H. Ito, "120-GHz-band millimeter-wave photonic wireless link for 10-Gb/s data transmission", IEEE Transactions on Microwave Theory and Techniques **54**, 1937 (2006)
4. P. Kužel and F. Kadlec, "Tunable structures and modulators for the THz light," Comptes Rendus de l'Académie des Sciences – Physique, (2007), in press.
5. J. Bae, H. Mazaki, T. Fujii, and K. Mizuno, "An optically controlled modulator using a metal strip grating on a silicon plate for millimeter and sub-millimeter wavelengths," IEEE Microwave Theory and Techniques Symposium **3**, 1239 (1996).
6. T. Nozokido, H. Minamide, and K. Mizuno, "Modulation of sub-millimeter wave radiation by laser-produced free carriers in semiconductors," Electron. Commun. Jpn. II **80**, 1 (1997).
7. S. Lee, Y. Kuga, and R. A. Mullen, "Optically tunable millimeter-wave attenuator based on layered structures," Microwave Opt. Technol. Lett. **27**, 9 (2000).
8. S. Biber, D. Schneiderbanger, and L.-P. Schmidt, "Design of a controllable attenuator with high dynamic range for THz-frequencies based on optically stimulated free carriers in high-resistivity silicon," Frequenz **59**, 141 (2005).
9. L. Fekete, J. Y. Hlinka, F. Kadlec, P. Kužel, and P. Mounaix, "Active optical control of the terahertz reflectivity," Opt. Lett. **30**, 1992 (2005).
10. L. Fekete, F. Kadlec, P. Kužel, and H. Němec, "Ultrafast opto-terahertz photonic crystal modulator," Opt. Lett. **32**, 680 (2007).
11. H.-T. Chen, W. J. Padilla, J. M. O. Zide, S. R. Bank, A. C. Gossard, A. J. Taylor, and R. D. Averitt, "Ultrafast optical switching of terahertz metamaterials fabricated on ErAs/GaAs nanoisland superlattices," Opt. Lett. **32** 1620 (2007).

#82782 - $15.00 USD Received 7 May 2007; revised 19 Jun 2007; accepted 19 Jun 2007; published 3 Jul 2007

12. C. Kadow, S. B. Fleischer, J. P. Ibbetwon, J. E. Bowers, A. C. G. J. Dong, and C. J. Palmstrom, "Self-assembled ErAs islands in GaAs: Growth and subpicosecond carrier dynamics," Appl. Phys. Lett. **75**, 3548 (1999).
13. H. Němec, L. Duvillaret, F. Quemeneur, and P. Kužel, "Defect modes due to twinning in one-dimensional photonic crystals," J. Opt. Soc. Am. B **21**, 548 (2004).
14. F. L. Pedrotti and L. S. Pedrotti, *Introduction to Optics*, 2nd ed. (Prentice Hall, Englewood Cliffs, 1993).
15. M. Born and E. Wolf, *Principles of Optics*, 7th ed. (University Press, Cambridge, 2003).
16. H. Němec, F. Kadlec, and P. Kužel, "Methodology of an optical pump-terahertz probe experiment: An analytical frequency-domain approach," J. Chem. Phys. **117**, 8454 (2002).
17. P. Kužel, F. Kadlec, and H. Němec, "Propagation of terahertz pulses in photoexcited media: analytical theory for layered systems," J. Chem. Phys. **127**, (2007), in press.
18. H. Němec, F. Kadlec, S. Surendran, P. Kužel, and P. Jungwirth, "Ultrafast far-infrared dynamics probed by terahertz pulses: a frequency domain approach. I. Model systems," J. Chem. Phys. **122**, 104503 (2005).
19. H. Němec, F. Kadlec, C. Kadlec, P. Kužel, and P. Jungwirth, "Ultrafast far-infrared dynamics probed by terahertz pulses: a frequency domain approach. II. Applications," J. Chem. Phys. **122**, 104504 (2005).

1. Introduction

Generation, detection and control of pulsed and continuous-wave terahertz (THz) radiation have received considerable attention during last years. Indeed, THz technology is a research field which has a growing impact *e.g.* on semiconductor and superconductor physics and on medical, space and defence industries [1]. As future short-range indoor communication systems may be designed for the sub-THz or THz range [2, 3] one can expect a growing emphasis put on the manipulation of both guided and freely propagating THz beams by means of agile switches, modulators, and phase shifters controlled either optically or electronically (see [4] for a review). Optically controlled THz switches or filters are of particular interest as they are in principle able to achieve ultrahigh speeds.

The THz properties of undoped semiconductors like Si or GaAs can be easily modified by optical pulses or cw radiation [5, 6, 7, 8, 9, 10]. These materials are transparent for the THz radiation in their ground states whereas the inter-band photoexcitation leads to the generation of free mobile carriers which induce a dramatic increase of absorption in the THz range. The lifetime of free carriers in optically controlled semiconductors determines the speed of the response. Semiconductors with a long free carrier lifetime (like Si) can be used as attenuators [8] controlled by a weak cw optical beam. This is possible because the photo-carrier density under continuous illumination is directly proportional to the lifetime. On the other hand, it has been pointed out [6, 9] that an appreciable level of tuning of the THz transmission in GaAs with sub-ns response is achieved only using quite intense pump pulses to reach the carrier concentration of $10^{17} - 10^{18}\,\mathrm{cm}^{-3}$.

An interesting possibility to increase the strength of the interaction of the THz radiation with free carriers is to incorporate the semiconductor plate or layer into a photonic crystal [10] or to use a metamaterial structure [11]. An efficient modulation of the THz beam with a response time of 100 ps was first demonstrated by using a structure consisting of a thin GaAs wafer embedded into a one-dimensional (1D) photonic crystal (PC) [10]. Subsequently, the authors of Ref. [11] have taken advantage of ultrafast properties of ErAs/GaAs multilayers [12] and of a two-dimensional (2D) electrically resonant metamaterial structure with sub-wavelength pattern. They have demonstrated THz switching capabilities of the structure at the photocarrier density level of $10^{16}\,\mathrm{cm}^{-3}$ with a response time of about 20 ps.

1D PCs have received a considerable attention because of the possibility of an analytical description of their behavior [13] and for the simplicity of their fabrication. Usually, a 1D PC consists of a stack of alternating dielectric layers of two materials with a high contrast of refractive indices and shows a forbidden band of frequencies where the transmission through the structure is inhibited. A defective 1D PC is constructed by inserting a defect layer (a GaAs wafer in our case) into the multilayer structure. For a suitable design, a localization of the THz

#82782 - $15.00 USD Received 7 May 2007; revised 19 Jun 2007; accepted 19 Jun 2007; published 3 Jul 2007

electric field close to the GaAs wafer occurs, which enhances its interaction with the photocarriers. An efficient modulation of the THz light is then achieved at substantially lower photoexcitation fluences [10]. Such structures are suitable for applications with quasi-monochromatic THz radiation because their operation bandwidth is reduced to the linewidth of the defect mode.

In this paper we study in detail several configurations of 1D PCs, both photoexcited and in the ground state. In particular, we propose a general model describing the time response of such PCs and the procedure of optimization of their parameters with respect to the speed of operation of the device and with respect to the resonant enhancement of its properties. An ultrafast response of our devices is demonstrated by using the optical pump—THz probe experimental technique.

2. Theoretical description

The PCs we used in our experiments consist of three blocks P, S and Q (see Fig. 1). These devices can be described as Fabry-Pérot resonators with two Bragg mirrors (blocks P and Q) enclosing a thin cavity made of GaAs in the middle (block S).

The THz spectrum of such a structure exhibits forbidden bands where the transmission is significantly reduced and so called defect modes inside those bands which are characterized by a high transmission coefficient. Our Bragg mirrors are composed of quarter-wave stacks of high-index (001)-oriented MgO plates (THz index $n_H = 3.12$, nominal thickness $d_H = 42 \pm 1\,\mu$m) and low-index (0001)-oriented crystalline quartz ($n_L = 2.10$, $d_L = 60 \pm 1\,\mu$m). The central wavelength of the lowest forbidden band is equal to $\lambda_c \equiv c/f_c = 2(n_L d_L + n_H d_H)$, where c is the speed of light in vacuum; in our case: $f_c \approx 0.58\,$THz. The defect layer in the middle of the structure is a GaAs platelet with an approximately half-wave optical thickness ($n = 3.55$, $d = 65 \pm 1\,\mu$m). The device operates at frequency $\omega_0 = 2\pi f_0$ corresponding to that of the defect mode in the lowest forbidden band ($f_0 \approx 600\,$GHz in all structures studied).

The materials of the Bragg mirrors are transparent for both optical and THz radiation. This is an important issue, *e.g.*, an absorption constant as low as 0.25 cm^{-1} at 600 GHz would lead to the drop of the amplitude transmission coefficient of the studied PCs in the ground state by a few per cent.

We investigate theoretically four symmetrical structures differing slightly by the sequence of layers composing the Bragg mirrors P and Q. The block P consists basically of 4 n_H-n_L bilayers and the block Q shows the reversed sequence of layers as compared to P; in other words, the block Q is the mirror image of the block P (see Fig. 1). We investigate the following structures:
(1) the block P is LHLHLHLHL (the structure is abbreviated as LHL);
(2) P is HLHLHLHL (abbrev. HL);
(3) P is LHLHLHLH (abbrev. LH);
(4) P is HLHLHLHLH (abbrev. HLH).
Besides that, non-symmetrical structures (different P and Q) are briefly discussed. The first two structures on the list were realized experimentally and the results of the measurements are analyzed within the models developed.

The principle of operation is such that the optical control pulse creates free carriers at the surface of the GaAs layer. These carriers disturb the resonant feedback of the photonic crystal in the THz range and dynamically reduce the THz transmittance of the structure at ω_0. In this section we calculate and discuss the response function of the device.

Note that we systematically distinguish between the frequencies f, f_p, Δf expressed in THz and angular frequencies ω, ω_p, $\Delta\omega$ in rad/ps, respectively, where $\omega = 2\pi f$, etc.

#82782 - $15.00 USD Received 7 May 2007; revised 19 Jun 2007; accepted 19 Jun 2007; published 3 Jul 2007

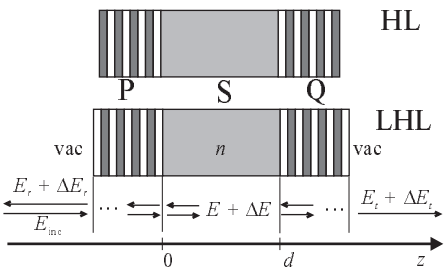

Fig. 1. Top: scheme of experimentally studied PC structures (the thicknesses of layers are out of scale); the sample consists of three blocks: P, S and Q, where S is the GaAs layer and the sequence of layers in the blocks P and Q differs for the two samples shown (n_L-layer is white; n_H-layer is dark). Bottom: notation introduced for the electric field in the photo-excited PC.

2.1. Response function of photo-excited PC

The optical properties of layered structures are usually described by the transfer matrix formalism [14, 15]. Our PCs consist of stacks of homogeneous layers with their normals parallel to the *z*-axis (see Fig. 1). The transfer matrices relate the tangential components of the electric and magnetic field at input and output interfaces, i.e.

$$\begin{pmatrix} E_{\text{in}} \\ \eta_0 H_{\text{in}} \end{pmatrix} = M \begin{pmatrix} E_{\text{out}} \\ \eta_0 H_{\text{out}} \end{pmatrix}, \tag{1}$$

where M is the appropriate transfer matrix. For the case of the normal incidence, the transfer matrix of a single homogeneous layer (e.g. of the defect layer S of the PC) reads:

$$S = \begin{pmatrix} \cos(nk_0 d) & i/n \sin(nk_0 d) \\ in \sin(nk_0 d) & \cos(nk_0 d) \end{pmatrix}; \tag{2}$$

n is the complex refractive index of the layer, d is its thickness, $k_0 = \omega/c$ is the wave vector in vacuum, and $\eta_0 = \sqrt{\mu_0/\varepsilon_0}$ is the vacuum wave impedance. The transfer matrix of the whole multi-layer stack equals the product of the transfer matrices of all constituents.

For any general layered structure (described by the components m_{ij} of its transfer matrix) surrounded by air the transmission (t) and reflection (r) coefficients read:

$$t = \frac{2}{m_{11} + m_{12} + m_{21} + m_{22}}, \qquad r = \frac{m_{11} + m_{12} - m_{21} - m_{22}}{m_{11} + m_{12} + m_{21} + m_{22}}. \tag{3}$$

The field distribution in the layer described by Eqs. (1) and (2) can be expressed as:

$$E(\omega; z) = E_{\text{in}}(\omega) \cos(nk_0 z) - i \frac{\eta_0 H_{\text{in}}(\omega)}{n} \sin(nk_0 z), \tag{4}$$

with $0 \leq z \leq d$.

The optical pump (or control) pulse generates free carriers in the semiconductor layer within its optical penetration depth. These carriers induce a transient conductivity $\Delta\sigma$ at THz frequencies which decays with the carrier lifetime.

In the steady-state approximation, *i.e.* assuming that the carrier recombination at the semiconductor surface is negligible within the time window of interest (¡ 1 ns), the transmission function of the photoexcited structure is considered to be time-independent and can be evaluated by using the standard transfer matrix formula 3 without any additional assumption.

#82782 - $15.00 USD Received 7 May 2007; revised 19 Jun 2007; accepted 19 Jun 2007; published 3 Jul 2007

Fast optical control of the defect layer of the PC can be treated in the framework of the formalism developed for the data analysis in optical pump—THz probe experiments [16, 17], as described below.

In communication applications the probing pulse is the pulse on which the optical control is to be exerted and, consequently, it may be long and quasi-monochromatic. Here we use time-resolved spectroscopy, *i.e.*, the probing THz pulse is usually short and broadband. In either case we define a time τ_p describing the delay between the excitation and probing pulse [16]. It has been shown that such a problem can be described and solved analytically in the frequency space (ω, ω_p), ω being the frequency of the THz pulse spectrum and ω_p being a "pump–probe" frequency conjugated to the time τ_p [16].

In this paper we refer to the photoinduced change ΔE of the THz field in the sample as to the transient THz field (see Fig. 1). This field is induced by the transient current Δj of photocarriers moving under the "applied" local THz field E. The propagation of $\Delta E(\omega, \omega_p; z)$ is then described by the following wave equation [16, 18]:

$$\frac{\mathrm{d}^2 \Delta E}{\mathrm{d}z^2} + n^2 k_0^2 \Delta E = i\eta_0 k_0 \Delta j(\omega, \omega_p; z)\,. \tag{5}$$

We assume that $\Delta E \ll E$; it then follows [17]:

$$\Delta j(\omega, \omega_p; z) = \exp[-(i\omega_p/v_g + \alpha)z] E(\omega - \omega_p; z) \Delta\sigma(\omega, \omega_p)\,, \tag{6}$$

where v_g is the group velocity of the optical beam in the sample layer and α is the optical linear absorption coefficient; E describes the THz electric field distribution in the structure in the ground state.

The photoexcited GaAs wafer shows the Drude behavior with a dominating contribution of free electrons, *i.e.* [18],

$$\Delta\sigma(\omega, \omega_p) = \frac{e^2 N_e}{m^*} \frac{1}{i\omega + 1/\tau_s + 1/\tau_c} \frac{1}{i\omega_p + 1/\tau_c}\,. \tag{7}$$

where τ_c is the free electron lifetime, τ_s is the electron momentum scattering time, e is the elementary charge, N_e and m^* are the free electron concentration and effective mass, respectively. Experimentally we found that $\tau_s/\tau_c \approx 10^{-3}$ implying that $1/\tau_s + 1/\tau_c \approx 1/\tau_s$ (see the experimental part for details). We point out that the frequency mixing in terms of $\omega - \omega_p$ in Eq. (6) is due to the fast response of the device. For a long free electron lifetime the transient susceptibility differs from zero in a close vicinity of $\omega_p = 0$ and vanishes rapidly at higher values of ω_p. In this case the frequency mixing can be neglected, *i.e.*, $E(\omega - \omega_p; z)$ can be replaced by $E(\omega; z)$ in Eq. (6). Nevertheless, we solve the problem for the general case which involves the frequency mixing effect.

Assuming that a THz wave E_{inc} impinges on the structure (see Fig. 1) the transfer matrix formalism allows us first to express the fields E_{in} and H_{in} at $z = 0$ and then to calculate the equilibrium field distribution in the GaAs plate with the help of Eq. (4). Subsequently, the field $E(\omega - \omega_p)$ is introduced into the expression for the transient current (6), the wave equation (5) is solved and the expression for the output transient wave $\Delta E_t(\omega, \omega_p)$ is found (see [17] for more details). This expression depends on the transmission and reflection properties of the building blocks of the structure which are adjacent to the thin photoexcited layer: $\tilde{r}_P$ and $\tilde{t}_P = t_P$ are the THz field reflectance and transmittance, respectively, of the block P surrounded by air obtained if the light impinges on the block from the right-hand side; r_{SQ} and t_{SQ} are the field reflectance and transmittance of the block SQ in air with the incident beam coming from the left-hand side. Assuming a strong optical absorption in the GaAs wafer ($\alpha \gg 1/L, k_0$), *i.e.*, the

#82782 - $15.00 USD Received 7 May 2007; revised 19 Jun 2007; accepted 19 Jun 2007; published 3 Jul 2007

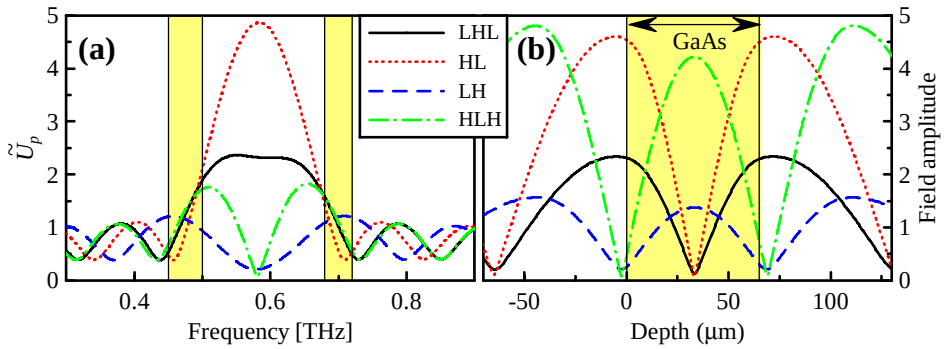

Fig. 2. (a) Spectral dependence of the enhancement factor $\tilde{U}_P$ for the structures discussed in the text. The yellow blocks approximately delimit the edges of the band gap (which is slightly different for the four structures). (b) Spatial profile of the THz electric field amplitude in the vicinity of GaAs defect (yellow block) at the defect mode frequency f_0.

optical penetration depth is small compared to the wafer thickness and to the THz wavelengths, one finds the following expression for the dynamical response of the PC to the photoexcitation:

$$\Delta E_t(\omega,\omega_p) = -\frac{\eta_0}{2\alpha}\,\tilde{U}_P(\omega)\,t(\omega)\,U_{SQ}(\omega-\omega_p)\,t(\omega-\omega_p)\,\Delta\sigma(\omega,\omega_p)E_{\rm inc}(\omega-\omega_p)\,, \qquad (8)$$

where t is the field transmittance of the whole PC and where the enhancement factors $\tilde{U}_P$ and U_{SQ} read:

$$\tilde{U}_P(\omega) = \frac{1+\tilde{r}_P(\omega)}{t_P(\omega)}\,, \qquad U_{SQ}(\omega-\omega_p) = \frac{1+r_{SQ}(\omega-\omega_p)}{t_{SQ}(\omega-\omega_p)}\,. \qquad (9)$$

2.2. Role of P and Q blocks

The modulation properties of the PC described by Eq. (8) depend on its equilibrium transmission function and on the properties of the blocks P and SQ. These terms will be analyzed below.

The transmission function $t(\Omega)$ of the entire structure (with $\Omega=\omega$ or $\omega-\omega_p$) is very small within the forbidden band with the exception of a narrow range around the defect mode frequency ($\Omega=\omega_0$). It is easy to show that no defect mode appears in the forbidden band if the periodicity of the photonic crystal is not broken by the defect: the transmission functions of the blocks t_P and t_{SQ} appearing in (9) exhibit a forbidden band without the defect mode. The corresponding field reflectances $\tilde{r}_P$ and r_{SQ} reach values close to either -1 or 1 inside the forbidden band.

In the former case ($\tilde{r}_P, r_{SQ}\approx -1$) the enhancement factors $\tilde{U}_P$ and U_{SQ} are smaller than 1 [at least close to the center of the forbidden band, see Fig. 2(a)] which means that the transmittance of the structure is rather insensitive to the photoexcitation (ΔE_t is small). This occurs when the high-index layers are adjacent to the defect in the PC (*i.e.* for structures HLH and LH). The physical arguments justifying these terms follow. We remind that the optical thickness of the GaAs defect in our structures is close to $\lambda_c/2$. For a half-wave thickness of the defect layer, $nd=(2m+1)\lambda_c/2$, the defect mode appears in the center of the band gap and the electric field profile has an even symmetry; for $nd=m\lambda_c$ the defect mode also appears in the center of the forbidden band but it has an odd symmetry [see Fig. 3(a)]. In both cases the modes show nodes at the edges of the defect layer where the free carriers are generated as shown in Fig. 2(b); consequently, the interaction is weak and the enhancement factors of the structures LH and

#82782 - $15.00 USD Received 7 May 2007; revised 19 Jun 2007; accepted 19 Jun 2007; published 3 Jul 2007

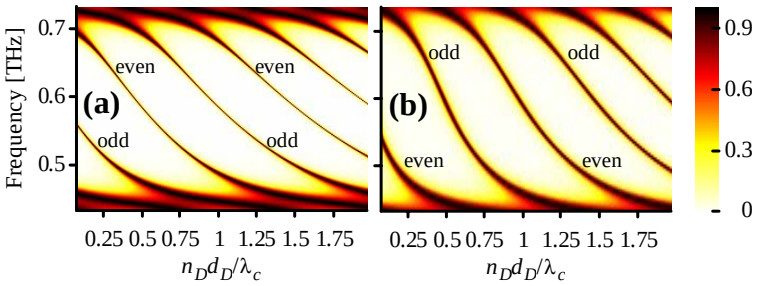

Fig. 3. Power transmittance of the structures HLH (a) and LHL (b) versus frequency and relative optical thickness of the defect. The transmittance level is represented by colors ($T = 1$ for black color and $T = 0$ for white color). Odd and even defect modes of the structure are identified.

HLH are very small close to the center of the forbidden band [Fig. 2(a)]. On the other hand, $\tilde{U}_P$ shows somewhat higher values close to the band gap edges for these structures. It is then possible to find in Fig. 3(a) some suitable thicknesses of the defect layer where an optically induced modulation could be observed. Nevertheless, this modulation is not very high and the close proximity of the forbidden band edges make these configurations less useful. It follows from this discussion that the structures with high-index layers adjacent to the defect are not suitable for opto-THz modulation.

In the latter case ($\tilde{r}_P, r_{SQ} \approx 1$), the terms $\tilde{U}_P$ and U_{SQ} reach values above 1 within the whole forbidden band as $t_p, t_{SQ} \ll 1$ [see Fig. 2(a)]. The investigated interaction is then enhanced owing to the field localization close to the defect layer (ΔE_t is big). This situation occurs if the layer adjacent to the defect in the P and Q blocks is the one with the low refractive index (*i.e.* for structures LHL and HL). The discussion is analogous to the one presented above; however, the symmetry of the modes is just the opposite one for each case of interest [Fig. 3(b)]. For example, in the case of a half-wave thickness of the defect plate, the defect mode in the center of the forbidden band exhibits an odd symmetry which implies anti-nodes at the edges of the defect leading to the enhancement of the opto-THz modulation (Fig. 2). The structures with a low-index layer adjacent to the defect are thus highly suitable for our purpose.

As pointed out above, the magnitude of the terms $\tilde{U}_P$ and U_{SQ} at the defect mode frequency is connected to the spatial distribution of the field in the defect layer, but it depends also on the strength of the field localization. This parameter depends on the number of periods of the PC and on the nature of the outermost layers at both sides of the PC: the n_L-layers (n_H-layers) at the boundary of PC significantly decrease (increase) the impedance mismatch between the structure and air and thus decrease (increase) the field enhancement.

We did not consider here explicitly non-symmetrical PCs (where the blocks P and Q of the structure are different). We just point out that for these structures the transmittance at the defect mode frequency is usually significantly reduced even in the ground state of the defect layer and, consequently, they are less suitable for applications.

Figure 4 shows the calculated effect of photo-excitation on the discussed symmetrical PCs in a steady-state limit, *i.e.*, without taking into account the time decay of the free carrier population. In this limit the transmission function of the PC can be calculated by using the exact formula 3 instead of 8 and the approximation $\Delta E \ll E$ need not to be fulfilled. Note that the structures LHL and HL show an appreciable modulation of the defect mode while the transmittance of the structure outside the band gap remains unaffected by photoexcitation. In contrast, for the structures HLH and LH, the photoexcitation influences the parts of the spectra in the close vicinity of the band gap edges instead of the defect mode in the center of the forbidden

#82782 - $15.00 USD Received 7 May 2007; revised 19 Jun 2007; accepted 19 Jun 2007; published 3 Jul 2007

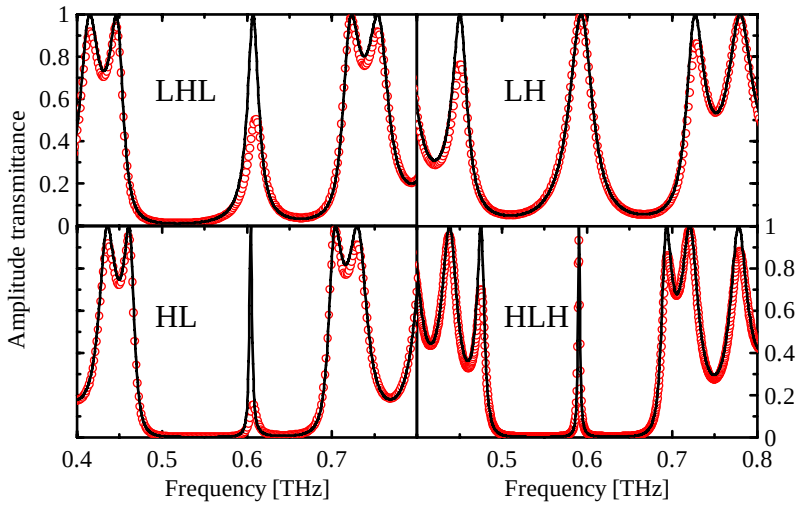

Fig. 4. Calculated THz spectra of four PCs. Lines: ground state; symbols: photoexcited state with a surface carrier density of $10^{16}\,\mathrm{cm}^{-3}$.

band. Precisely this behavior was predicted in the above discussion.

The HL structure is expected to show the best performance for the optical control of the THz propagation as it exhibits the highest field localization at the photoexcited layer. However, the field localization at the defect layer is closely related to the quality factor of the structure defined as the ratio of the defect mode frequency f_0 and the full-width-at-half-maximum (FWHM) Δf of its spectral line. It results that a strong enhancement leads to a reduction of Δf and to a slowing down of the device response. A compromise thus should be found between the speed of the device and the enhancement factor. This issue will be discussed in the next paragraph which deals with the time response of the PC.

2.3. Dynamical response of the PC

The dynamical response of the PC upon photoexcitation is described by Eq. (8). It consists of the structural response of the PC given by the products

$$\tilde{X}_P(\omega) = \tilde{U}_P(\omega)t(\omega), \qquad X_{SQ}(\omega-\omega_p) = U_{SQ}(\omega-\omega_p)t(\omega-\omega_p) \tag{10}$$

and of the material response of photoexcited GaAs given by the photoconductivity $\Delta\sigma(\omega,\omega_p)$.

In this paragraph we consider merely the structures LHL and HL, where the transmission at the defect mode frequency can be efficiently modulated. These structures show high values of the enhancement factors $\tilde{U}_P$ and U_{SQ} inside the band gap, which makes the parts of the spectra outside the band gap relatively unimportant for this analysis. Indeed, the spectra $\tilde{X}_P$ and X_{SQ} show sharp high maxima at $\omega=\omega_0$ and $\omega-\omega_p=\omega_0$, respectively, and do not reach high values outside the forbidden band. In the vicinity of the defect mode frequencies, the expressions (10) can be approximated by

$$\tilde{X}_j(\Omega) \approx \tilde{U}_j(\omega_0)t(\omega_0)\,\frac{\exp[-i(\Omega-\omega_0)\tau_0]}{1+i(\Omega-\omega_0)\tau_{\mathrm{PC}}} \tag{11}$$

(see Fig. 5), where j stands for P or SQ, $\Omega=\omega$ or $\omega-\omega_p$ and where, for a given symmetrical structure, the parameters τ_{PC}, τ_0 and ω_0 acquire the same values for $\tilde{X}_P$ and X_{SQ}. The parameter

#82782 - $15.00 USD Received 7 May 2007; revised 19 Jun 2007; accepted 19 Jun 2007; published 3 Jul 2007

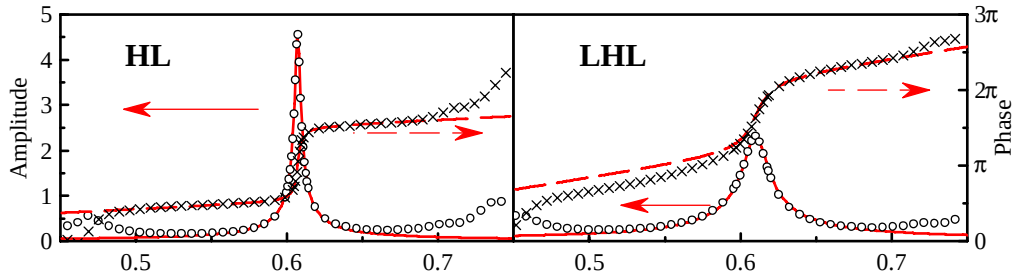

Fig. 5. Spectral functions $\tilde{X}_P$ defining the structural part of the dynamical response of the PCs for HL and LHL structures. The symbols were calculated by using the transfer matrix formalism and the structural and optical data of the PCs; the lines correspond to the best approximation using Eq. (11). Very similar plots are found also for X_{SQ} with the same values of parameters τ_{PC}, τ_0 and ω_0.

τ_{PC} can be interpreted as the lifetime of the THz wave inside the resonator and it can be easily shown that $\tau_{\mathrm{PC}} = 1/(\pi\Delta f)$, where Δf is the full width at half maximum (FWHM) of the defect mode in the power transmittance spectrum. The time τ_0 reaches very small values for our samples—0.47 and 1.54 ps for HL and LHL structures, respectively—we did not find any simple physical interpretation of this parameter and it has practically no importance taking into account the resolution of about 1 ps in our experiments.

Going back to Eq. (11), one finds similar sharp maxima also at the defect mode frequencies in higher order band gaps. In Fig. 6 we plot a 2D map of the dynamical response in the (ω,ω_p) space for the LHL structure. Figure 6a shows in fact the quantity $\Delta E_t(\omega,\omega_p)/[E_{\mathrm{inc}}(\omega-\omega_p)\Delta\sigma(\omega,\omega_p)]$ describing the structural part of the response of the device. The same response is obtained for an ultrafast semiconductor where τ_s, $\tau_c \to 0$ such that $\Delta\sigma(\omega,\omega_p) = const$ in the frequency range studied. In this plot the contributions from higher order band gaps are clearly observed: see the side maxima at $f_p \approx \pm 1.2$ THz. This would enable a strong frequency mixing in Eq. (8) where high values of ω_p would play an important role.

On the other hand, if the peak in $\Delta\sigma$ versus ω_p is narrower than the width of the forbidden band of the photonic structure, the side maxima in the 2D plot with $\omega_p \neq 0$ are suppressed. This is illustrated in Fig. 6(b) where the spectrum of $\Delta\sigma$ calculated for our sample from optical pump—THz probe measurements of the GaAs platelet placed out of the PC was used: the only significant signal comes from a narrow range at $\omega_p \approx 0$.

Two important applications of our model will be discussed here; each of them can be described by a specific cut in the (ω, ω_p) plane.

2.4. Application I: modulation of a monochromatic THz wave

The first experimental situation corresponds to the potential application of our device in the communication technology: the incident THz radiation is a monochromatic wave with frequency ω_0 and its output intensity is controlled by optical pulses. We wish to evaluate the time-dependent THz transmission of the structure upon a single photoexcitation event.

In this case, the spectrum of the incoming radiation is described by the Dirac δ-function:

$$E_{\mathrm{inc}}(\omega-\omega_p) = E_{\mathrm{inc}}\,\delta(\omega-\omega_p-\omega_0)\,, \tag{12}$$

which means that the probing event is delocalized in time. The value of τ_p in this experiment is undetermined and can be arbitrarily chosen, most conveniently $\tau_p = 0$. The response of the PC

#82782 - $15.00 USD Received 7 May 2007; revised 19 Jun 2007; accepted 19 Jun 2007; published 3 Jul 2007

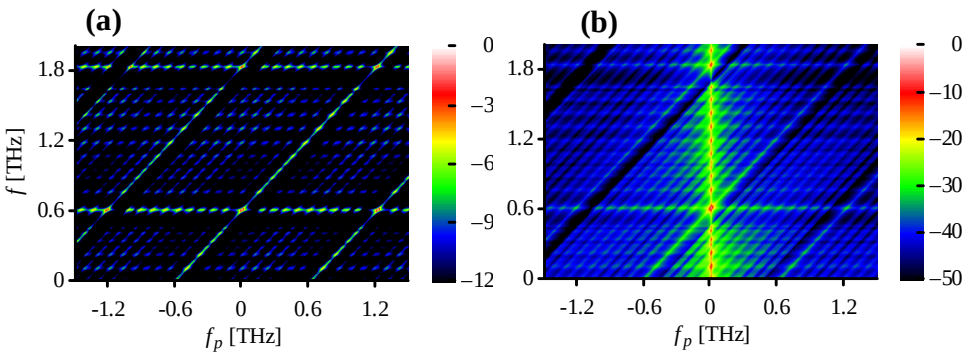

Fig. 6. Dynamical response of the LHL structure expressed by the function $\Delta E_t(\omega,\omega_p)/E_{\rm inc}(\omega-\omega_p)$ in the (ω,ω_p) space. The function is normalized to unity and its amplitude is plotted in the logarithmic scale. (a) $\Delta\sigma(\omega,\omega_p)=const$ in the plotted range; this is obtained for an ultrafast semiconductor with a response faster than 1 ps. The sharp maxima correspond to defect modes in several forbidden bands. (b) $\Delta\sigma(\omega,\omega_p)$ is given by Eq. (7) with time constants corresponding to our GaAs wafer. The response coming from higher-order forbidden bands is strongly suppressed and the only appreciable signal comes from the close vicinity of $\omega_p=0$.

then reads:

$$\Delta E_t(\omega)=-\frac{\eta_0 e^2 N_e}{2\alpha m^*}E_{\rm inc}\frac{t(\omega_0)U_{SQ}(\omega_0)}{i\omega+1/\tau_s}\,\frac{\tilde{X}_P(\omega)}{i(\omega-\omega_0)+1/\tau_c}\,. \tag{13}$$

The time-dependent intensity of the radiation transmitted through the photoexcited PC is then given by

$$I(\tau)=\left|\Delta E_t(\tau)+E_{\rm inc}\,t(\omega_0)\,\exp(i\omega_0\tau)\right|^2. \tag{14}$$

Using the approximation of the defect mode expressed by Eq. (10) one finds:

$$I(\tau=\tilde{\tau}+\tau_0)\approx|t(\omega_0)|^2 I_{\rm inc}\left|Y(\tilde{\tau})\,B\,\frac{\exp(-\tilde{\tau}/\tau_{\rm PC})-\exp(-\tilde{\tau}/\tau_c)}{1-\tau_{\rm PC}/\tau_c}+1\right|^2 \tag{15}$$

where Y is the Heaviside step function and

$$B=\frac{\eta_0 e^2 N_e}{2\alpha m^*}\,\frac{t(\omega_0)\tilde{U}_P(\omega_0)U_{SQ}(\omega_0)}{i\omega_0+1/\tau_s}\,. \tag{16}$$

The results of this calculation are shown in Fig. 7 for typical sets of parameters. In the ground state, the resonator dynamically stores a part of THz electromagnetic energy. The photoexcitation event makes the input port opaque and the stored energy is depleted with the lifetime $\tau_{\rm PC}$; therefore the switch-on time is equal to $\tau_{\rm PC}$ as predicted by (15). The feedback is restored with the lifetime τ_c of free electrons in GaAs which equals the switch-off time of the modulation. The magnitude of the modulation depends on the ratio $\tau_{\rm PC}/\tau_c$: for $\tau_c<\tau_{\rm PC}$ the modulation depth is significantly reduced. The width of the modulation pulse at one half of its maximum in Fig. 7(a) is 330 ps for the HL structure and 200 ps for the LHL structure.

We note that, following our model, a 100 ps long modulation pulse could be achieved using the LHL structure and a hypothetical semiconductor with the carrier lifetime of 70 ps. In this case the free carrier density of $10^{16}\,{\rm cm}^{-3}$ in a 750 nm thick surface layer of the semiconductor should lead to about 42% modulation depth of the THz output power.

#82782 - $15.00 USD Received 7 May 2007; revised 19 Jun 2007; accepted 19 Jun 2007; published 3 Jul 2007

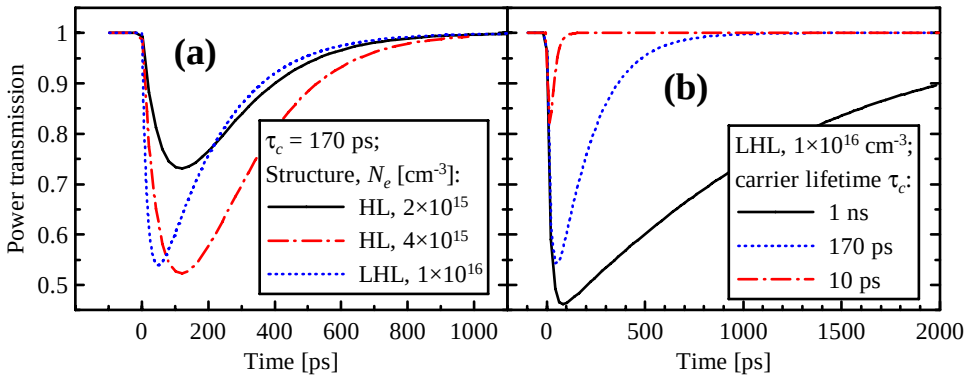

Fig. 7. Power transmission $I(\tau)$ of the PCs at ω_0 after a photoexcitation event occurring at time $\tau = 0$. (a) Carrier lifetime: $\tau_c = 170$ ps, momentum scattering time: $\tau_s = 160$ fs; initial concentration of photocarriers N_e and structure parameters are varied. (b) $N_e = 1 \times 10^{16}$ cm^{-3}; τ_c is varied.

2.5. *Application II: Optical pump—THz probe experiment*

The second case discussed here is that of a pump–probe experiment. The incident THz radiation is an ultrashort pulse. The time-resolved signal is monitored at the resonant frequency ω_0 as a function of the pump–probe delay τ_p. The frequency domain signal reads:

$$\Delta E_t(\omega_0,\omega_p) = -\frac{\eta_0 e^2 N_e}{2\alpha m^*} E_{\rm inc}(\omega_0-\omega_p)\frac{t(\omega_0)\tilde{U}_P(\omega_0)}{i\omega_0+1/\tau_s}\frac{\tilde{X}_{SQ}(\omega_0-\omega_p)}{i\omega_p+1/\tau_c}. \quad (17)$$

It is important to note that the spectrum of THz pulses is broad and smooth, therefore it can be considered as constant close to ω_0, *i.e.*, $E_{\rm inc}(\omega_0-\omega_p)\approx E_{\rm inc}$. This model is expected to describe accurately our THz time-resolved experiments (see below). Taking into account Eq. (11), one finds after a 1D inverse Fourier transformation and using the substitution $\tilde{\tau}_p = \tau_p + \tau_0$:

$$\Delta E_t(\omega_0,\tau_p=\tilde{\tau}_p-\tau_0) = -\frac{t(\omega_0)E_{\rm inc}B}{1+\tau_{\rm PC}/\tau_c}\left[Y(\tilde{\tau}_p)\exp(-\tilde{\tau}_p/\tau_c)+Y(-\tilde{\tau}_p)\exp(\tilde{\tau}_p/\tau_{\rm PC})\right]. \quad (18)$$

Note that the pump-probe signal does not vanish for small negative delays. Indeed, since the THz pulse is stored in the resonator during the time $\tau_{\rm PC}$, the delayed pump pulse can still control the PC output during this time. Thus for negative pump-probe delays the signal increases with $\tau_{\rm PC}$ while for positive delays the signal decreases with the decay of free carriers.

For short carrier lifetimes the pump–probe signal is diminished due to the term $1+\tau_{\rm PC}/\tau_c$ in the denominator. Indeed, if $\tau_c \lesssim \tau_{\rm PC}$ the density of free carriers significantly decreases during their interaction with the THz pulse inside the structure. This term then can be understood as an effective renormalization $N_{\rm eff}$ of the initial carrier density N_e taking into account the dynamical parameters of the structure:

$$N_{\rm eff} = \frac{N_e}{1+\tau_{\rm PC}/\tau_c}. \quad (19)$$

3. Experiment and Results

3.1. *Experimental setup*

PC samples were characterized by time-domain THz spectroscopy using a standard transmission setup for steady-state measurements and an optical pump—THz probe setup [19] for

#82782 - $15.00 USD Received 7 May 2007; revised 19 Jun 2007; accepted 19 Jun 2007; published 3 Jul 2007

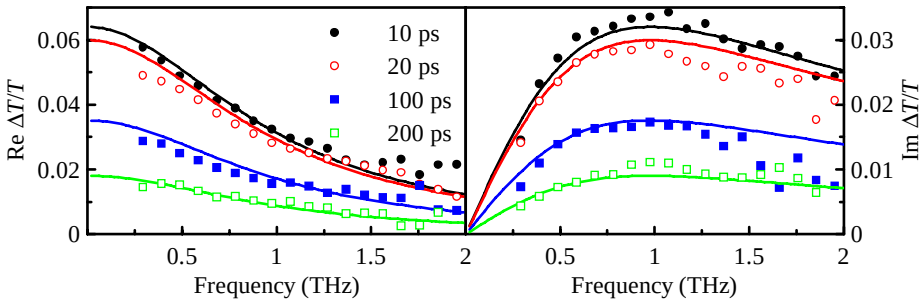

Fig. 8. Transient THz spectra of a GaAs:Cr wafer (used later as a defect in photonic structures) obtained at several pump–probe delays indicated in the legend. Symbols: experimental data; lines: fits by a Drude model using $N_e = 1.5 \times 10^{16}\,\mathrm{cm}^{-3}$, $\tau_s = 160\,\mathrm{fs}$ and $\tau_c = 170\,\mathrm{ps}$.

measurements of photoexcited samples. As a laser source we used an amplified laser system (Quantronix, Odin) which provides 55-fs-long pulses with the repetition rate of 1 kHz with the wavelength of 810 nm and the energy in pulse of 1 mJ. The pulses were split into three branches; all of them were equipped with delay lines for a precise adjustment of pulses arrivals. The pulses in the first and second branches were used for the generation and gated detection of the THz radiation via optical rectification and electro-optic sampling scheme, respectively, using two identical 1-mm-thick [011]-oriented ZnTe crystals. The generated THz pulses were focused onto the sample by an ellipsoidal mirror; the transmitted THz radiation was then directed to the ZnTe sensor by using another ellipsoidal mirror.

The third branch was utilized for the optical excitation of the samples. The intensity of excitation was varied by a pair of neutral gradient filters. To ensure a homogenous excitation of the samples the pump beam diameter was stretched by an optical telescope to approximately 12 mm. The holder of the PC samples had a clear aperture of 4 mm, which was larger than the diameter of the focused THz beam spot.

3.2. Experimental results

The structure of investigated PCs was described at the beginning of the theoretical description. The defect layer was an optically polished weakly chromium doped GaAs wafer. The photocarriers in this wafer show a Drude-like behavior as measured by optical pump—THz probe spectroscopy. In Fig. 8 the momentum scattering time τ_s determines the shape of the transient THz spectra and the carrier lifetime τ_c controls their decay with pump–probe delay. For the photocarrier concentrations around $10^{16}\,\mathrm{cm}^{-3}$ we found $\tau_s = 160 \pm 5\,\mathrm{fs}$ and $\tau_c = 170 \pm 10\,\mathrm{ps}$. These values are related to the doping by chromium.

The lengths of time-domain scans were typically 200–250 ps yielding a spectral resolution of 4–5 GHz. Each steady-state spectrum was obtained as a ratio of Fourier transforms of a wave form E transmitted through an unexcited PC and a reference wave form E_{ref} (measured with an empty aperture). These spectra are shown in Fig. 9(a) and (aa) for the LHL and HL structure, respectively. The transfer matrix calculations of the structure with GaAs in the ground state give a good account of the experiments. We slightly adjusted the nominal thicknesses of GaAs and MgO to match exactly the measured defect mode frequency and the forbidden band edges: we used $d = 64.5\,\mu\mathrm{m}$ and $d_H = 42.7\,\mu\mathrm{m}$ to obtain $f_0 = 609\,\mathrm{GHz}$ for the LHL structure and $f_0 = 606\,\mathrm{GHz}$ for the HL structure. The linewidth of the defect mode gives access to τ_{PC}. However, one should realize that the apparent THz resonator lifetime $\tilde{\tau}_{\mathrm{PC}}$ as measured in our

#82782 - $15.00 USD Received 7 May 2007; revised 19 Jun 2007; accepted 19 Jun 2007; published 3 Jul 2007

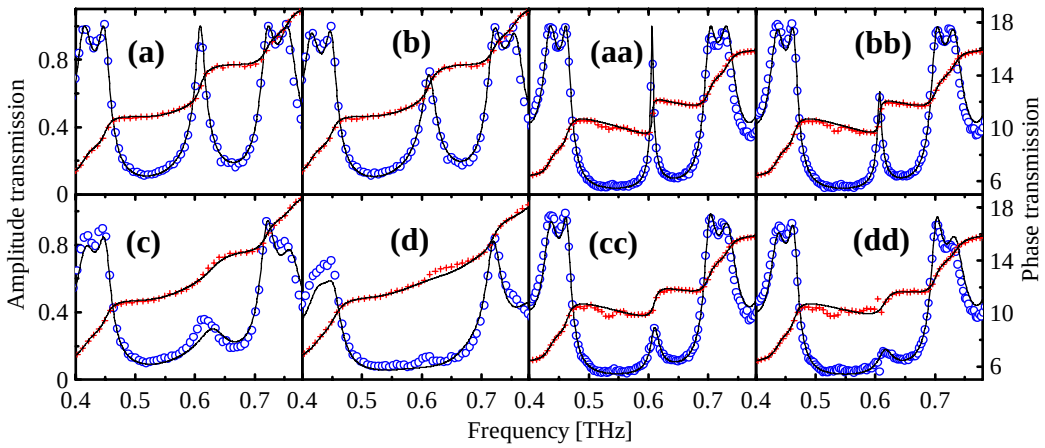

Fig. 9. Examples of amplitude (circles) and phase (crosses) transmittance of samples in LHL (a–d) and HL (aa–dd) configuration as a function of the pump pulse fluence: LHL:(a) $0\,\mu\mathrm{J/cm^2}$ (ground state), (b) $0.4\,\mu\mathrm{J/cm^2}$, (c) $2.4\,\mu\mathrm{J/cm^2}$. (d) $8.0\,\mu\mathrm{J/cm^2}$; HL: (aa) $0\,\mu\mathrm{J/cm^2}$ (ground state), (bb) $0.24\,\mu\mathrm{J/cm^2}$, (cc) $0.9\,\mu\mathrm{J/cm^2}$, (dd) $2.0\,\mu\mathrm{J/cm^2}$. The pump-probe delay is 5 ps. Lines correspond to the data calculated by using the transfer matrix formalism.

experiments is obtained as

$$\frac{1}{\tilde{\tau}_{\mathrm{PC}}} \approx \frac{1}{\tau_{\mathrm{PC}}} + \frac{1}{\tau_{\mathrm{L}}} + \frac{1}{\tau_{\mathrm{W}}}, \tag{20}$$

where τ_{L} is the lifetime due to extinction losses in the structure (essentially related to the residual absorption of the layers, to the scattering on the interfaces and in microcavities between the layers and to the divergence of the THz beam) and $\tau_{\mathrm{W}} \approx 250\,\mathrm{ps}$ is the length of the window in the time domain measurement. We found from the experiment: $\tilde{\tau}_{\mathrm{PC}} = 19.5 \pm 0.5\,\mathrm{ps}$ (LHL) and $\tilde{\tau}_{\mathrm{PC}} = 60 \pm 2\,\mathrm{ps}$ (HL). This is in excellent agreement with the theory which provides: $\tau_{\mathrm{PC}} = 20\,\mathrm{ps}$ (LHL) and $\tau_{\mathrm{PC}} = 85\,\mathrm{ps}$ (HL). This result shows that our structures have a very good optical quality as their extinction losses are quite small ($\tau_{\mathrm{L}} > 1\,\mathrm{ns}$).

In experiments with the pump beam on, our setup allows us to measure the photoinduced change $\Delta E(t)$—called transient wave form—with a high sensitivity (Fig. 10). The actual wave form transmitted through the photoexcited sample is then calculated as the sum $E(t) + \Delta E(t)$.

The response of HL and LHL samples was studied for different excitation fluences varying from $0.4\,\mu\mathrm{J/cm^2}$ to $8\,\mu\mathrm{J/cm^2}$ for the LHL structure and from $0.08\,\mu\mathrm{J/cm^2}$ to $2\,\mu\mathrm{J/cm^2}$ for the HL structure. The corresponding transmission spectra are shown in Fig. 9. In the time domain, the transient wave forms obtained at low pump fluences show quasi-monochromatic oscillations at f_0 [as observed in the inset of Fig. 10(b)] damped approximately with the time constant τ_{PC}. This proves that the photoexcitation modifies the transmission principally at the defect mode frequency. At other frequencies the transmission is influenced only weakly [curves (b), (bb), (c) and (cc) in Fig. 9]. For the high pump fluence limit [curves (d) and (dd)] the defect mode is entirely suppressed.

The solid lines in these figures are calculated using the steady-state transfer matrix formalism. In these calculations a linear absorption process of the pump beam in GaAs with absorption coefficient $\alpha = 1.3\,\mu\mathrm{m}^{-1}$ was assumed. Using the transfer matrix formalism for the 810 nm pump beam we have evaluated that about 75 % of the incident power (which is directly measured) is absorbed in the GaAs wafer. From this value it is possible to estimate the surface density of free carriers N_e for any pump fluence. The complex THz refractive index of pho-

#82782 - $15.00 USD Received 7 May 2007; revised 19 Jun 2007; accepted 19 Jun 2007; published 3 Jul 2007

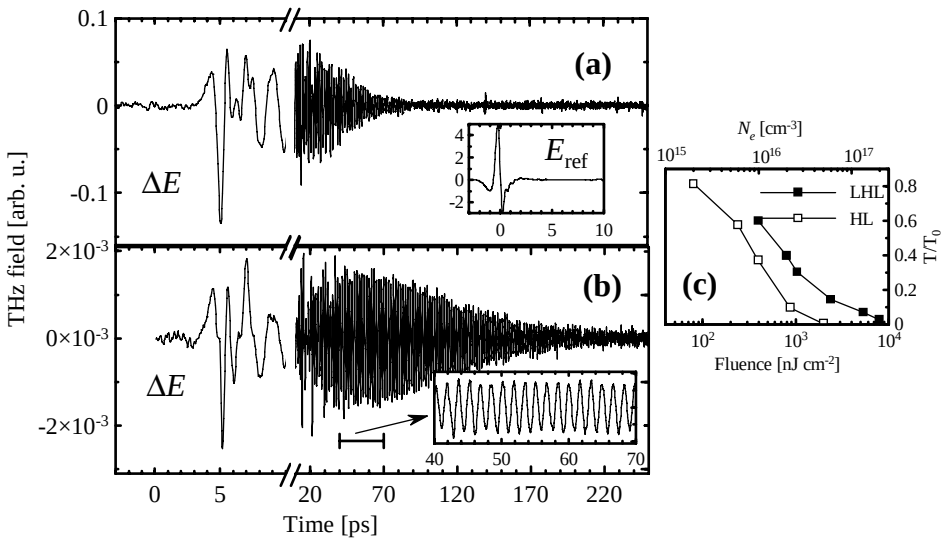

Fig. 10. Examples of transient THz wave forms ΔE for a pump–probe delay $\tau_p = 5\,\mathrm{ps}$. (a) LHL structure, pump fluence: $0.8\,\mu\mathrm{J/cm^2}$; (b) HL structure, pump fluence: $0.24\,\mu\mathrm{J/cm^2}$. Inset in (a): reference wave form; Inset in (b): 30-ps-long detail of the wave form. (c) Ratio T/T_0 between the power transmission of the PCs in photoexcited and ground state at the defect mode frequency versus the incident fluence and surface carrier density. The line is a guide for the eye.

toexcited GaAs is then evaluated by using the Drude conductivity model, in which, in order to account for the finite carrier lifetime and in agreement with our findings in the theoretical part of this paper, the value of effective electron concentration N_{eff} defined by Eq. (19) is taken for the actual carrier density. The agreement between the experimental and theoretical spectra is very good for both samples and all pump fluences provided that the values of incident pump fluences estimated from the experimental conditions are systematically divided by a factor of 1.4 in these calculations. This discrepancy can be explained by optical power losses due to interferences in micron-sized air cavities between the constituent layers of the PC and by a small error in the calibration of the powermeter used to estimate the pump fluence. After this correction we obtain that a carrier density of $N_e = 1 \times 10^{16}\,\mathrm{cm^{-3}}$ is achieved with a fluence of $0.4\,\mu\mathrm{J/cm^2}$. The variation of the transmitted power at the defect mode frequency as a function of the pump fluence and/or free carrier concentration is shown in Fig. 10(c). We also evaluated the amplitude of $\Delta E_t(\omega_0, \tilde{\tau}_p \approx 0)$ by using Eq. (18) and verified that it matches well (within 2%) the drop of the transmittance at the defect mode frequency for the lowest pump fluences shown in Figs. 9(b) and (bb).

The transient wave forms were studied as a function of the pump–probe delay for both LHL and HL structures. The time-resolved response at ω_0 for a low pump fluence shown in Fig. 11 is in very good agreement with the theory expressed by Eq. (18). We find decay times of 160 ps (HL) and 180 ps (LHL) which are to be compared to the carrier lifetime of 175 ps, and the rise times of 60 ps (HL) and 18.5 ps (LHL) which match very well the values of the apparent resonator lifetime $\tilde{\tau}_{PC}$.

From the point of view of applications the issue of narrow-range tuning of the defect mode frequency is important. Tilting the crystal with respect to the THz beam axis leads to a small increase of the defect mode frequency. In our experiments we have studied the response of the LHL structure between 0 and 25 degrees and observed a shift of the defect mode by 8.5 GHz.

#82782 - $15.00 USD Received 7 May 2007; revised 19 Jun 2007; accepted 19 Jun 2007; published 3 Jul 2007

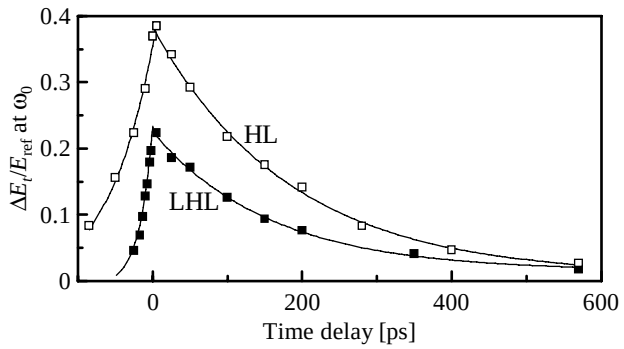

Fig. 11. The rise and decay of the photo-induced signal $\Delta T = \Delta E_t/E_{\rm ref}$ at the defect mode frequency for the two structures studied. Pump pulse fluence: $0.4\,\mu$J/cm^2; points: measured data; solid lines fit by expression (18).

By tilting the sample by 25 degrees the power transmittance dropped by about 20%.

4. Conclusion

We have studied in detail the THz dynamics of one-dimensional photonic crystals with a GaAs defect layer upon photoexcitation and their potential for the optical modulation of the THz radiation. Optimum resonant structures were selected and constructed. Their dynamical response is determined by the photocarrier lifetime (switch-off time) and by the resonator lifetime of THz photons (switch-on time). The experimental results are in excellent agreement with the theoretical predictions. The pump pulse energies necessary to induce a 50% modulation of the THz power are comparable to those delivered by current commercial femtosecond oscillators; the time response of our modulators is faster than 330 ps. The bit rate of these elements is then determined by the femtosecond oscillator repetition rate.

Acknowledgment

This work was supported by the Grant Agency of Academy of Sciences of the Czech Republic (project No. KJB100100512) and by the Ministry of Education of the Czech Republic (project No. LC512).

#82782 - $15.00 USD Received 7 May 2007; revised 19 Jun 2007; accepted 19 Jun 2007; published 3 Jul 2007